Downregulation of *IL16* Expression Induces Chemotherapeutic Drug Sensitivity via Increased Degradation of Mutant *TP53* in Acute Myeloid Leukemia Cells

Heng Zhang[1]*, Pengfei Qin[1]*, Anqiao Li[1], Zhenqian Huang[1], Sida Peng[1], Haiming Li[1], Lihua Xu[1,2]

[1]Department of Hematology, The First Affiliated Hospital of Guangzhou Medical University, Guangzhou, China
[2]Guangdong Key Laboratory of Urology, The First Affiliated Hospital of Guangzhou Medical University, Guangzhou, China
*These authors contributed equally to this work

Background: Interleukin 16 (*IL16)* is a pleiotropic cytokine that does not belong to any interleukin family and functions as a $CD4^+$ T-cell chemokine, a regulator of T-cell activation, and an inhibitor of human immunodeficiency virus replication in acquired immunodeficiency syndrome. Studies in the hemato-oncological disease multiple myeloma have demonstrated that *IL16* plays an important role in promoting tumor cell growth and is associated with tumor burden and prognosis. However, the role of *IL16* in acute myeloid leukemia (AML) remains largely unexplored.

Aims: To investigate the potential role of *IL16* in AML.

Study Design: *In vitro* experiments.

Methods: Bioinformatic analyses were conducted using online databases, including gene expression profiling interactive analysis 2, to evaluate *IL16* expression and its prognostic significance in patients with AML. Transcriptome data from AML samples were used for gene function enrichment analysis, gene set enrichment analysis (GSEA), survival analysis, and other related bioinformatic assessments. In addition, a single-cell dataset was analyzed using the R programming language to identify specific *IL16* expression subgroups in AML patients. The expression and secretion of *IL16* in various AML cell lines were assessed using Western blot and ELISA. *IL16* knockdown AML cell lines were generated and evaluated for proliferation, apoptosis, and multidrug resistance to chemotherapy using cell-based assays and protein immunoblotting to determine the effects of *IL16* on AML biological behavior. Furthermore, transcriptome sequencing analysis was performed to elucidate the molecular mechanisms underlying the effects of *IL16* on the biological functions of AML cells.

Results: *IL16* expression levels were significantly elevated in patients with AML and were associated with poorer prognosis. *IL16* was predominantly expressed in T cells, malignant hematopoietic stem cells, malignant progenitor cells, and malignant mononuclear precursor cells in AML patients. Knockdown of *IL16* expression significantly inhibited proliferation and promoted chemotherapy-induced apoptosis in AML cells *in vitro*. Downregulation of *IL16* also reduced cell viability and decreased the IC50 of cytarabine (Ara-C) across different concentrations. Furthermore, reduced *IL16* expression may induce degradation of mutated *TP53* in AML cells, resulting in increased apoptosis and enhanced sensitivity to multiple chemotherapeutic agents.

Conclusion: High *IL16* expression was observed in malignant cells from patients with AML. Downregulation of *IL16* promotes degradation of mutant *TP53* and induces apoptosis, thereby increasing the sensitivity of AML cells to various chemotherapeutic agents *in vitro*.

Corresponding author: Sida Peng, Department of Hematology, The First Affiliated Hospital of Guangzhou Medical University, Guangzhou, China

e-mail: hgcore@126.com

Corresponding author: Haiming Li, Department of Hematology, The First Affiliated Hospital of Guangzhou Medical University, Guangzhou, China

e-mail: lihaiming@gzhmu.edu.cn

Corresponding author: Lihua Xu, Department of Hematology, The First Affiliated Hospital of Guangzhou Medical University; Guangdong Key Laboratory of Urology, The First Affiliated Hospital of Guangzhou Medical, University, Guangzhou, China

e-mail: xlhua@gzhmu.edu.cn

Received: January 3, 2026 **Accepted:** March 12, 2026 • **DOI:** 10.4274/balkanmedj.galenos.2026.2025-12-245

Available at www.balkanmedicaljournal.org

ORCID iDs of the authors: H.Z. 0009-0006-3372-9828; P.Q. 0000-0002-7546-7380; A.L. 0009-0001-8424-1543; Z.H. 0009-0005-1677-9340; S.P. 0009-0003-9418-4014; H.L. 0009-0004-0831-313X; L.X. 0000-0002-3437-1286.

Cite this article as: Zhang H, Qin P, Li A, et al. Downregulation of *IL16* Expression Induces Chemotherapeutic Drug Sensitivity via Increased Degradation of Mutant *TP53* in Acute Myeloid Leukemia Cells.. Balkan Med J.;

INTRODUCTION

Acute myeloid leukemia (AML) is a highly heterogeneous hematological malignancy with poor prognostic outcomes and significant treatment challenges.[1] Current therapeutic approaches primarily include chemotherapy, allogeneic hematopoietic stem cell (HSC) transplantation, and targeted small-molecule therapies. The National Cancer Institute estimates that around 20,000 individuals will be diagnosed with AML in 2023, and approximately 10,000 will die from AML-related complications.[2] Survival and prognosis for patients with AML are improving as existing treatment options continue to be optimized and with the advent of chimeric antigen receptor T-cell immunotherapy. However, some patients still have difficulty achieving a complete response (CR), and relapse after CR or develop chemotherapy resistance; therefore, there is an urgent need to discover effective targets for targeted therapy.

Interleukin 16 (*IL16*) is an independent proinflammatory cytokine.[3,4] It is synthesized as a precursor protein, pro-*IL16*, with an apparent molecular weight of 80 kDa. Following various cellular stimuli, pro-*IL16* is cleaved by caspase 3 (CASP3) into a secreted carboxyl-terminal peptide with a molecular weight of 17 kDa and an amino-terminal 60 kDa prestructural domain.[5-7] The former is the functional extracellular *IL16*, whereas the latter enters the nucleus and influences the cell cycle. It is primarily secreted by activated $CD8^+$ T lymphocytes, mast cells, and macrophages.[8] *IL16* is secreted into plasma as a ligand for CD4/CD9 and functions as a chemokine, growth factor, and differentiation factor for a variety of hematopoietic cell types involved in specific autoimmune and inflammatory responses.[9] Its function is largely dependent on surface expression and signaling through $CD4^+$ cells.[10-12]

In multiple hematological oncology studies, *IL16* has been characterized as a proinflammatory cytokine involved in immune dysregulation in patients with hematologic malignancies. In patients with diffuse large B-cell lymphoma, *IL16* has been shown to be a biological marker of treatment response.[13] Single-cell transcriptomic profiling of mixed phenotype acute leukemia samples revealed notable activation of *IL16* signaling pathways, along with cytokine–cytokine receptor interactions and interferon-alpha signaling via the Janus kinase-signal transducer and activator of transcription pathway axis in relapsed cases. These data implicate these pathways in leukemogenesis and are correlated with adverse clinical outcomes.[14-16] These findings indicate that *IL16* may influence the tumor immune microenvironment in hematologic malignancies by promoting the expression of inflammation-related pathways and may be associated with stress, drug resistance, and poor prognosis. While *IL16* has been investigated in various hematologic malignancies, existing research has predominantly focused on lymphomas, which are tumors of lymphoid origin. In contrast, its functional significance in AML, a malignancy arising from the myeloid lineage, remains poorly defined. Given the distinct cellular origins and pathobiology of AML, we hypothesize that *IL16* contributes to chemotherapy resistance in this disease. To test this hypothesis, we designed the present study to elucidate the role and mechanism of *IL16* in AML drug resistance.

MATERIALS AND METHODS

Bioinformatics analysis

The Cancer Genome Atlas (TCGA) and Therapeutically Applicable Research to Generate Effective Treatments (TARGET) RNA-seq data with AML were acquired from The University of California, Santa Cruz (UCSC) Xena database (Table 1). A preliminary analysis of the differential expression of the *IL16* gene in the TCGA database was performed using the gene expression profiling interactive analysis 2 (GEPIA2) online platform.[17] AML transcriptome datasets from TCGA and TARGET were downloaded from the UCSC Xena database, and the clinical features were plotted in R. Statistical mapping for survival analysis was performed using GraphPad Prism software, and correlation analysis in R ($R > 0.4$) was used to filter relevant genes.[18] Gene function was then analyzed using the Metascape database, including enrichment and gene set enrichment analysis (GSEA) analysis.[19] The GSE116256 single-cell transcriptome dataset was downloaded from the Gene Expression Omnibus (GEO) database.[20]

Cell lines and culture conditions

AML cell lines (HL60, HEL, NB4, and THP1) were purchased from the Cell Bank of the Chinese Academy of Sciences. Cells were cultured in Roswell Park Memorial Institute 1640 medium with 10% FBS (HyClone; Cytiva) and maintained at 37 °C in a humidified incubator with 5% CO_2.

Construction of IL16 knockdown AML cell lines in vitro

AML cells were transduced using lentiviral infection. *IL16* scramble, sh1, sh2, and sh3 lentiviruses were purchased from Cyagen (Cyagen US Inc., CA, USA). The target sequences were: sh1: GTTCTGGATGAAGCAACATTA; sh2: CCAGTGATGTTTCTGTAGAAT; sh3: CCAATGGCACTCCCAAAGTTT.

Western blot analysis

Cells were lysed in RIPA lysis buffer (Beyotime Institute of Biotechnology, Shanghai, China), and protein concentration was determined using a bicinchoninic acid protein assay Kit. Proteins were separated on 10% and 12% sodium dodecyl sulfate-polyacrylamide gel electrophoresis gels and transferred to polyvinylidene fluorid membranes (EMD Millipore, USA) blocked with 5% skim milk. Membranes were incubated overnight with primary antibodies, followed by secondary antibodies for 1 hour at room temperature. Protein bands were visualized using ECL solution.

RT-qPCR

RNA was extracted using TRIzol® reagent, and cDNA was synthesized from each RNA sample using the PrimeScript™ RT reagent Kit. Quantitative polymerase chain reaction (PCR) was performed using iQ™ SYBR® Green Supermix on the CFX384 Real-Time System (both from Bio-Rad Laboratories, Inc., Shanghai, China). The mRNA expression levels of *IL16* and glyceraldehyde-3-phosphate dehydrogenase (GAPDH) were quantified using the following primers: *IL16* forward: CAAGGAAGGGGCATCTCCAA, reverse: AGCTCTGAAAGGTTGAGCGA; GAPDH forward: AGGGGCCATCCACAGTCTT,

reverse: AGCCAAAAGGGTCATCATCTCT. The relative expression ratio was calculated using the $2^{-\Delta\Delta Cq}$ method.

Cell proliferation assay

Cell proliferation was measured using the Cell Counting Kit-8 (CCK-8; TransGen Biotech Co., Ltd., Beijing, China) according to the manufacturer's instructions. Cells were seeded at 1,000 cells per well in 96-well plates. 10 **µL of** CCK-8 solution was added every 24 hours, followed by a 2-hour incubation. Absorbance was measured at 450 nm.

Mitochondrial membrane potential assay

To assess early apoptosis, mitochondrial membrane potential was measured in *IL16*-knockdown AML cells using JC-1 staining after azacitidine (AZA) treatment. The depolarization ratio was calculated as the green/red fluorescence intensity ratio using confocal microscopy.

Cell cytotoxicity assay

Cytotoxicity was assessed using a CCK-8 assay. Cells seeded in 96-well plates were treated with various drugs for 48 hours. After adding CCK-8 and incubating for 2 hours, absorbance at 450 nm was measured to determine cell viability. Data from three independent experiments were analyzed using GraphPad Prism 8.

Nested PCR

Amplification of HL60 and THP1 cDNA for *TP53* mutations was performed using nested PCR. The first round of PCR was conducted with forward primer CCCCTCTGAGTCAGGAAACA and reverse primer TTATGGCGGGGAGGTAGACTG. The second round of PCR used forward primers GTCCCAAGCAATGGGATGATT and TGGCCATCTACAAGCAGTCA, and reverse primers CATAGGGCACCACCACACTA and TGAGTTCCAAGGCCTCATTC. PCR products were analyzed by agarose gel electrophoresis to confirm the expected band size, and correctly sized bands were sent to Sangon Biotech for sequencing and sequence analysis.

Cycloheximide (CHX) pulse-chase assay

The half-life of mutant *TP53* proteins was investigated using a cycloheximide (CHX) pulse-chase assay.[21] Cells were transfected with scramble shRNAs or shIL16. Seventy-two hours after transfection, cells were treated with CHX (100 µg/mL) for 0, 6, 12, 24, 40, and 48 hours. Mutant *TP53* protein levels were analyzed by Western blot using an anti-*TP53* antibody.

Statistical analysis

All statistical analyses were conducted using R version 4.5.2 (with the Seurat, tidyverse, multtest, dplyr, ggplot2, and patchwork packages) and GraphPad Prism. Data are presented as mean ± standard deviation, unless otherwise indicated. A two-sided p value < 0.05 was considered statistically significant. Kaplan–Meier survival curves were generated based on overall survival data. Differences between survival curves (high vs. low *IL16* expression groups) were assessed using the log-rank test. Hazard ratios (HRs) and 95% confidence intervals (CIs) were estimated from univariate Cox proportional hazards models. Associations between continuous variables were evaluated using Pearson's correlation coefficient. Cell viability data from CCK-8 assays across a range of drug concentrations were fitted to a non-linear regression model in GraphPad Prism. IC_{50} values and their 95% CI were interpolated from the fitted curves. Statistical comparisons of IC_{50} values between groups were performed using an extra sum-of-squares F test. Transcriptome sequencing and primary bioinformatic analyses were performed by Sangon Biotech Co. (Service Contract No. MRNA236020GZ). GSEA was performed using GSEA software v4.3.2. RNA-seq and GSEA results were evaluated using the normalized enrichment score and false discovery rate (FDR) q value, with FDR $q < 0.05$ used to identify significantly enriched biological pathways. For hypothesis-driven validation experiments (western blot, RT-qPCR, and cell cytotoxicity assays) that tested a limited set of predefined targets, nominal p values were used without adjustment for multiple comparisons. Comparisons between two groups were preceded by normality assessment using the Shapiro–Wilk test. However, we acknowledge that, with very small sample sizes, the power of normality tests is limited, and results should be interpreted with caution. Sample sizes were determined based on standard criteria routinely used to detect reproducible biological effects.

RESULTS

IL16 expression is upregulated and associated with poor prognosis in AML

GEPIA2 pan-cancer bioinformatics analysis revealed that the *IL16* gene is highly expressed in AML (Figure 1a, b). Further analysis of transcriptomic data from AML patients in the TCGA and TARGET datasets, obtained via the UCSC Xena database, showed that biological functions positively correlated with *IL16* expression ($R > 0.4$) were primarily enriched in the regulation of T-cell activity, immune responses, and cytokine-chemokine signaling. Functional enrichment analyses based on Gene Ontology and Kyoto Encyclopedia of Genes and Genomes (KEGG) further indicated that *IL16* expression is positively associated with immune modulation as well as cytokine and chemokine regulatory pathways (Figure 1c, d). Based on *IL16* expression levels and the survival outcomes and clinical characteristics of patients in the TCGA and TARGET AML transcriptomic datasets, we classified AML patients into high-expression and low-expression groups. Analysis of the TCGA and TARGET databases confirmed that age at diagnosis was a universal and stable independent adverse prognostic factor (TCGA: HR = 1.03, 95% CI: 1.02–1.05, $p < 0.001$; TARGET: HR = 1.06, 95% CI: 1.02–1.10, $p = 0.004$). The established disease risk stratification systems also demonstrated strong prognostic predictive ability in this study. For example, compared with the low-risk group, the death risk of the high-risk group was significantly increased (TARGET: HR = 4.56, 95% CI: 1.44–14.47, $p = 0.01$). In cytogenetic analysis, compared with the good-risk group, the unclassified (not otherwise specified) risk group had an extremely high-risk (HR = 27.73, 95% CI: 5.37–143.27, $p < 0.001$), although this result should be interpreted cautiously due to its wide CI. Notably, high *IL16* expression showed a hazard ratio associated with an adverse survival trend in both cohorts (TCGA HR = 1.17, 95% CI: 0.71–1.94, $p = 0.533$; TARGET

HR = 1.41, 95% CI: 0.92–2.17, $p = 0.115$), but none reached statistical significance ($p > 0.05$). This suggests that *IL16* may be a potential biomarker, warranting further investigation with a larger sample size (Supplementary Table 1). *IL16* expression in TCGA and TARGET AML transcriptome data was divided into high- and low-expression groups and further analyzed using GSEA software. Our study revealed significant enrichment of immunosuppressive, cytokine, and chemokine pathways in the high-expression group ($p < 0.01$, FDR q value < 0.01, NES > 2), indicating that these pathways are activated with increased *IL16* expression (Supplementary Figure 1a).

The IL16 gene is predominantly expressed in malignant tumor cells of AML patients

We obtained the single-cell RNA sequencing dataset GSE116256 from the GEO database. Cell clustering and annotation were performed using the Human Primary Cell Atlas as a reference. Columnar percentages of various cell types in normal HSCs and AML patient HSCs were compared, revealing a significant increase in myeloid cells in AML HSCs. Subsequent analysis of *IL16*-expressing HSCs revealed a predominance of malignant tumor cells (Figure 2a, b). Additionally, the expression of the known *IL16* ligand, CD4, was mainly observed

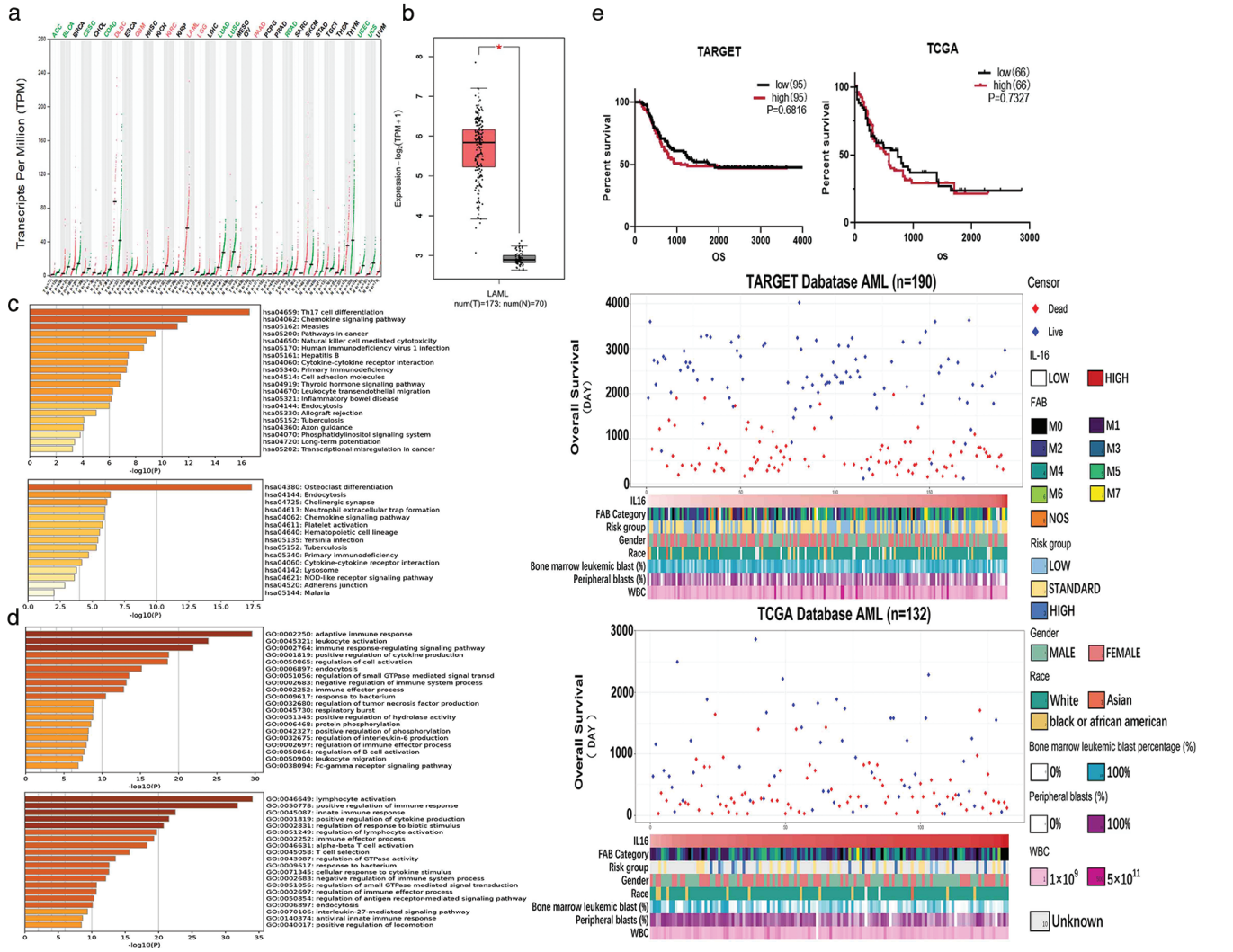

FIG. 1. *IL16* gene is highly expressed in AML patients, with higher expression levels correlating with poorer prognosis. (a, b) GEPIA2 online bioinformatic analysis demonstrates elevated *IL16* gene expression across various malignant tumors. (c, d) Correlation analysis was conducted using the R programming language to identify related genes (R > 0.4), followed by gene function enrichment analysis using the Metascape database. (e) Kaplan–Meier curves showing outcomes of AML patients from the TCGA and TARGET. Scatterplots were used to reflect the survival of AML patients. Heat maps were used to reflect clinical information about AML patients in the TCGA (n = 132) and TARGET (n = 190) datasets. (TCGA HR = 1.17, 95% CI: 0.71 - 1.94, $p = 0.533$; TARGET HR = 1.41, 95% CI: 0.92 - 2.17, $p = 0.115$).

IL16, interleukin 16; AML, acute myeloid leukemia; GEPIA2, gene expression profiling interactive analysis 2; HR, hazard ratio; CI, confidence interval; TCGA, The Cancer Genome Atlas; TARGET, Therapeutically Applicable Research to Generate Effective Treatments.

in monocytes within AML HSCs. Further analysis indicated that *IL16*-expressing cell subpopulations were primarily T cells, monocytes, monocyte precursors, and granular monocyte precursors (Figure 2c, d). Subpopulations of HSCs expressing *IL16* showed significantly elevated expression in malignant HSCs, malignant progenitor cells (Prog), and malignant granulocyte-macrophage progenitor cells, with notable statistical differences (Figure 2b). We then assessed *IL16* expression at both the mRNA and protein levels in four AML cell lines (NB4, HL60, THP1, and HEL). HEL exhibited the highest mRNA expression, whereas HL60 showed the lowest. At the protein level, NB4 had the highest *IL16* expression, while HEL had the lowest. Only NB4 displayed a distinct band at 16 kDa, whereas no corresponding bands were observed in the other cell lines under normal culture conditions without external stimuli (Figure 2e). The inconsistent mRNA and protein expression levels observed among the four AML cell lines may be attributed to distinct post-transcriptional modifications regulated differently in each cell line.

Chemotherapeutic drugs induce IL16 mRNA expression and promote cleavage of the IL16 precursor in AML cells

Two AML cell lines, HL60 and THP1, were treated with the chemotherapeutic drug AZA at 10 μM, which induced apoptosis. Following treatment, *IL16* mRNA expression was upregulated, and 16 kDa active *IL16* was detected by Western blot at 24 and 48 h, suggesting that apoptosis in AML cells may trigger CASP3-mediated cleavage of precursor *IL16*. This process leads to the release of active *IL16* along with apoptotic cells (Figure 2f). Previous studies have indicated that in CD8+ T lymphocytes, the *IL16* precursor is cleaved by CASP3 into a C-terminal domain of approximately 17 kDa and an N-terminal domain of 60 kDa. The C-terminal domain forms a mature *IL16* monomer of 130 amino acid residues, which is secreted extracellularly and covalently polymerized to form a biologically active homotetramer. These data suggest that a similar mechanism may exist in AML cells. In AML patients, malignant tumor cells predominantly accumulate in the myeloid lineage rather than the lymphoid lineage. Literature indicates that current research on *IL16* primarily focuses on the lymphoid lineage. Our study further found that functional *IL16* can be released from tumor cells along with apoptosis when stimulated by chemotherapeutic drugs. Based on these observations, we hypothesize that *IL16* can serve as a biomarker of aggressive disease in AML and may be involved in chemotherapy resistance.

Downregulation of IL16 promotes chemotherapy-induced apoptosis in AML cell lines

We established stable *IL16* knockdown cell lines, along with scramble controls, in HL60 and THP1 cells using lentiviral infection. The knockdown efficiency of *IL16* was verified at both mRNA and protein levels, confirming the efficacy of the shRNA1 construct (Figure 3a, b). Functional assays were then conducted using the knockdown and scramble cell lines.

The CCK8 proliferation assay revealed a significant decrease in cell viability at 24, 48, 72, and 96 h in the knockdown group compared with the scramble control in THP1 cells, whereas no significant differences were observed in HL60 cells (Figure 3c). After 24 h of coincubation with AZA, mitochondrial membrane potential was assessed in HL60 and THP1 cells. A significant decrease in mitochondrial membrane potential was observed in *IL16* knockdown cells compared with scramble controls. This reduction, indicative of early apoptosis, suggests that *IL16* downregulation may enhance early apoptosis in AZA-treated cells (Figure 3d, e). Given these findings, it is valuable to investigate whether *IL16* knockdown can also enhance apoptosis in response to other commonly used clinical chemotherapeutic agents, potentially overcoming resistance in AML cells.

Knockdown of IL16 overcome chemotherapy resistance in AML cells

To assess the role of *IL16* in chemotherapy-induced apoptosis, scramble control and *IL16*-shRNA HL60 and THP1 cells were treated with a range of concentrations of four chemotherapeutic agents: Ara-C, Ida, AZA, and Ven. *IL16* knockdown significantly reduced cell viability across multiple drug concentrations in both cell lines compared with controls. Furthermore, the IC_{50} for cell viability was markedly lower in *IL16*-deficient cells, indicating enhanced chemosensitivity (Figure 4a, Supplementary Table 2). Ara-C, Ida, AZA, and Ven are commonly used in the clinical treatment of AML and play critical roles in patient management. Our experimental data indicate that *IL16* may contribute to AML tumor cell resistance to various chemotherapeutic drugs. Subsequently, HL60 and THP1 cells in both the scramble and knockdown groups were treated with AZA at 10 μM for 0, 12, 24, and 48 h to assess the expression of apoptosis-related molecules via Western blot. Compared with controls, cleaved CASP3 (cCASP3) expression in HL60 cells significantly increased at different time points after treatment, with similar results observed in THP1 cells (Figure 4b). HL60 and THP1 cells were also treated with the targeted drug Ven. Compared with controls, cCASP3 levels significantly increased at different time points. Additionally, PARP cleavage, a marker of apoptosis, was significantly enhanced after Ven treatment. Notably, the degree of PARP cleavage in *IL16*-deficient cells was significantly higher than in controls at 6 and 12 h, further confirming the enhanced induction of apoptosis following *IL16* knockout (Figure 4c). Chemotherapy-induced apoptosis was evaluated using multiple complementary assays, including mitochondrial membrane potential measurement, CCK-8 cytotoxicity testing, and Western blot analysis of apoptosis-related proteins. All methods consistently demonstrated an enhanced apoptotic trend following *IL16* knockdown in both cell lines. These results suggest that *IL16* downregulation potentiates chemotherapy-induced apoptosis *in vitro*.

Downregulation of IL16 affects multiple biological processes in AML cells

To further elucidate the mechanisms underlying *IL16* downregulation as a strategy to overcome chemoresistance, transcriptome sequencing was performed on HL60 cells transfected with scramble or *IL16*-shRNA, followed by bioinformatic analysis. Differential gene expression analysis revealed that *IL16* knockdown resulted in 642 upregulated and 1,779 downregulated genes compared with the scramble control group (Figure 4d). KEGG pathway analysis showed

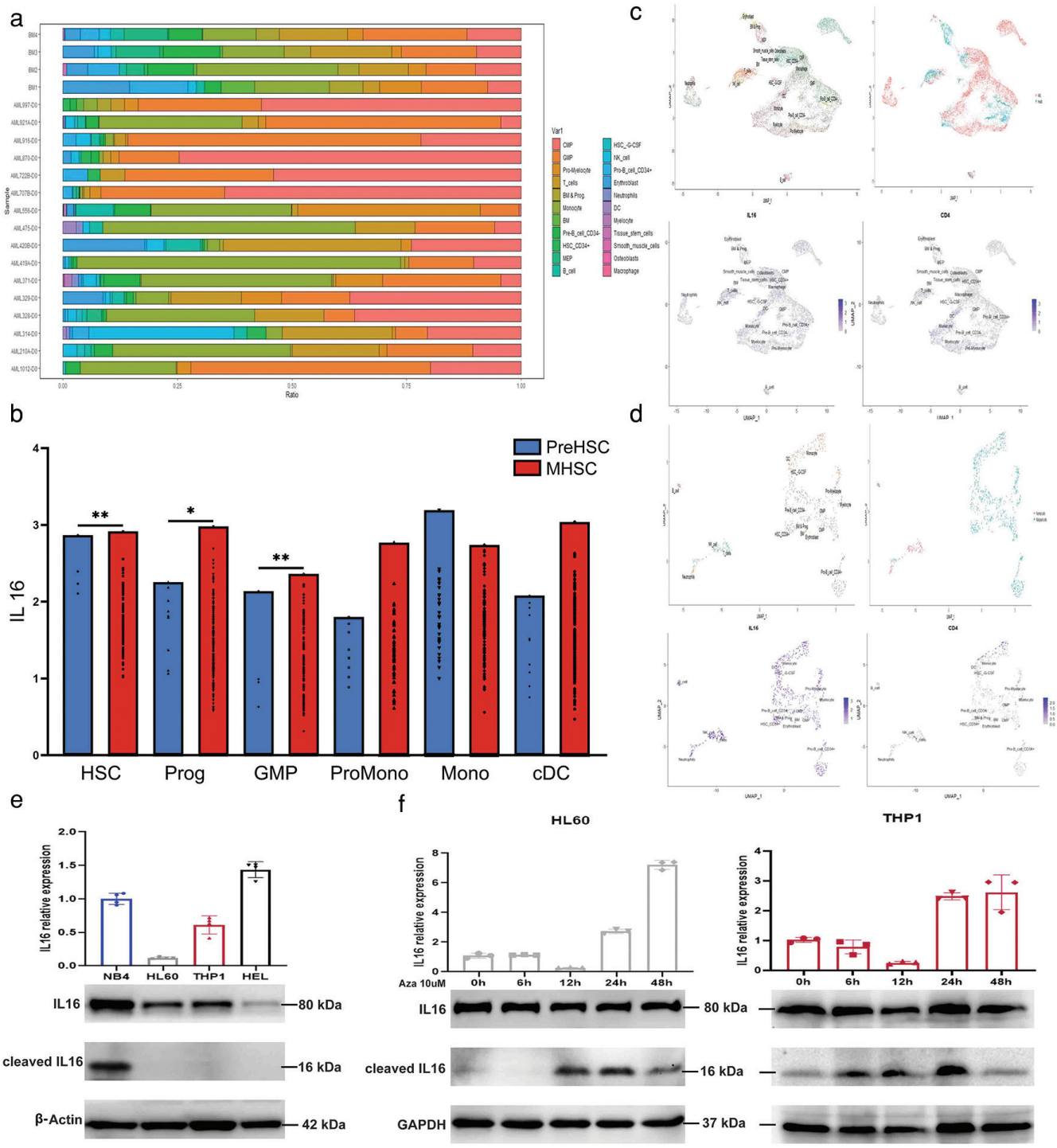

FIG. 2. The *IL16* gene is predominantly expressed in malignant tumor cells of AML patients. (a) Based on the HPCA database for clustering and annotation, the columnar occupancy of different cells was plotted for 4 normal donors and 16 AML patients. (b) Histogram of differences between presumed normal hematopoietic stem cells (PreHSC n = 783) and malignant hematopoietic stem cells (MHSC n = 880) expressing *IL16* under different clusters. Mann Whitney test * < 0.05 ** < 0.01. (c) UMAP projection of BM cells from nine patients with sixteen AMLs and four HDs, showing the formation of 22 main clusters. (d) UMAP projection of *IL16*-BM cells from bone marrow cells expressing *IL16*, showing the formation of 17 main clusters. (e) RT-qPCR and western blot detection of *IL16* in AML cell lines NB4 HL60 THP1 HEL. (f) mRNA and Protein expression levels were detected by RT-qPCR and Western blot after 0, 6, 12, 24 and 48 h co-incubation of AZA and AML cell lines HL60 and THP1. *IL16*, interleukin 16; AML, acute myeloid leukemia; BM, bone marrow; RT-qPCR, reverse transcription quantitative polymerase chain reaction; AZA, azacitidine.

that the affected functions were mainly enriched in the P53 pathway, apoptosis pathway, mitochondrial autophagy pathway, and MAPK pathway (Figure 4e). KOG analysis indicated that the differentially expressed genes were primarily associated with cell motility, signal transduction mechanisms, and cell cycle control, cell division, and chromosome partitioning (Figure 4f). Given the clinically observed association between *TP53* mutations and poor therapeutic outcomes, including frequent chemotherapy resistance, we hypothesized that *IL16* contributes to chemoresistance by modulating the stability of mutant *TP53* protein. To explore this mechanistic correlation, we designed subsequent molecular experiments for verification.

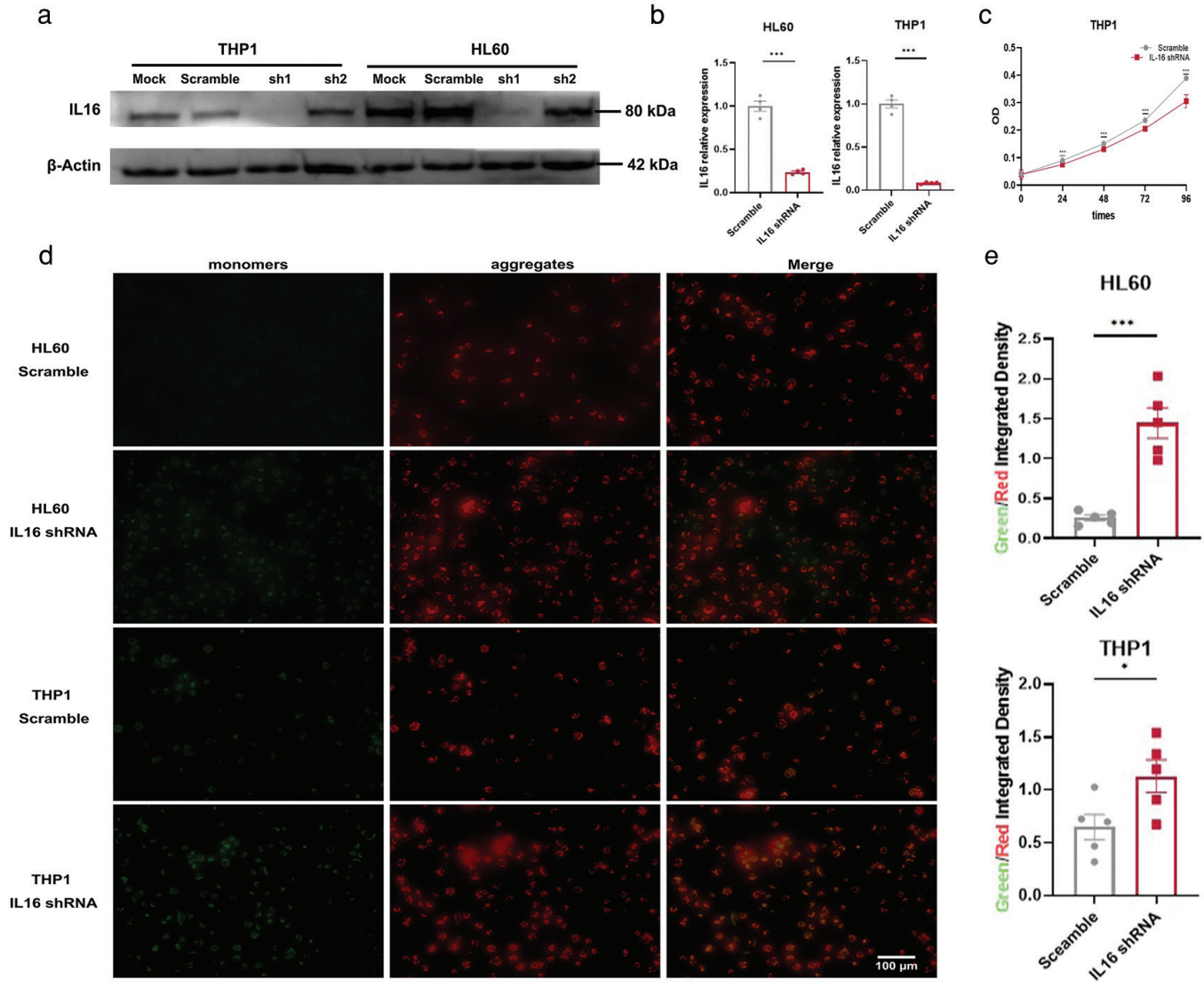

FIG. 3. Downregulation of *IL16* expression promotes chemotherapy-induced apoptosis in AML cell lines. (a, b) mRNA and protein levels of *IL16* in AML cells (THP1 and HL60) transfected with vector scramble or *IL16* shRNA were quantified by RT-qPCR and western blot analysis, respectively. Bar chart shows mRNA expression of scramble and *IL16* shRNA expressing. (c) Proliferation curves of THP1 scramble and *IL16* shRNA cell lines. At 24 h (p = 0.00086), 48 h (p = 0.000034), 72 h (p = 0.000034), and 96 h (p = 0.000007). (d) HL60 and THP1 *IL16* shRNA and scramble groups cells were separately treated with AZA for 24 h then mitochondrial membrane potential (JC-1) was measured by confocal microscopy (×100 uM). Red fluorescence means normal cells. Green fluorescence cells indicate loss of mitochondrial membrane potential. (e) Bar charts show expression levels as JC-1 Green/Red intensity with mean ± SD, n = 5, 5 randomly selected fields of view. Mann-Whitney U test *$p < 0.05$ **$p < 0.01$, *** $p < 0.001$.

IL16, interleukin 16; AML, acute myeloid leukemia; AZA, azacitidine; SD, standard deviation; RT-qPCR, reverse transcription quantitative polymerase chain reaction.

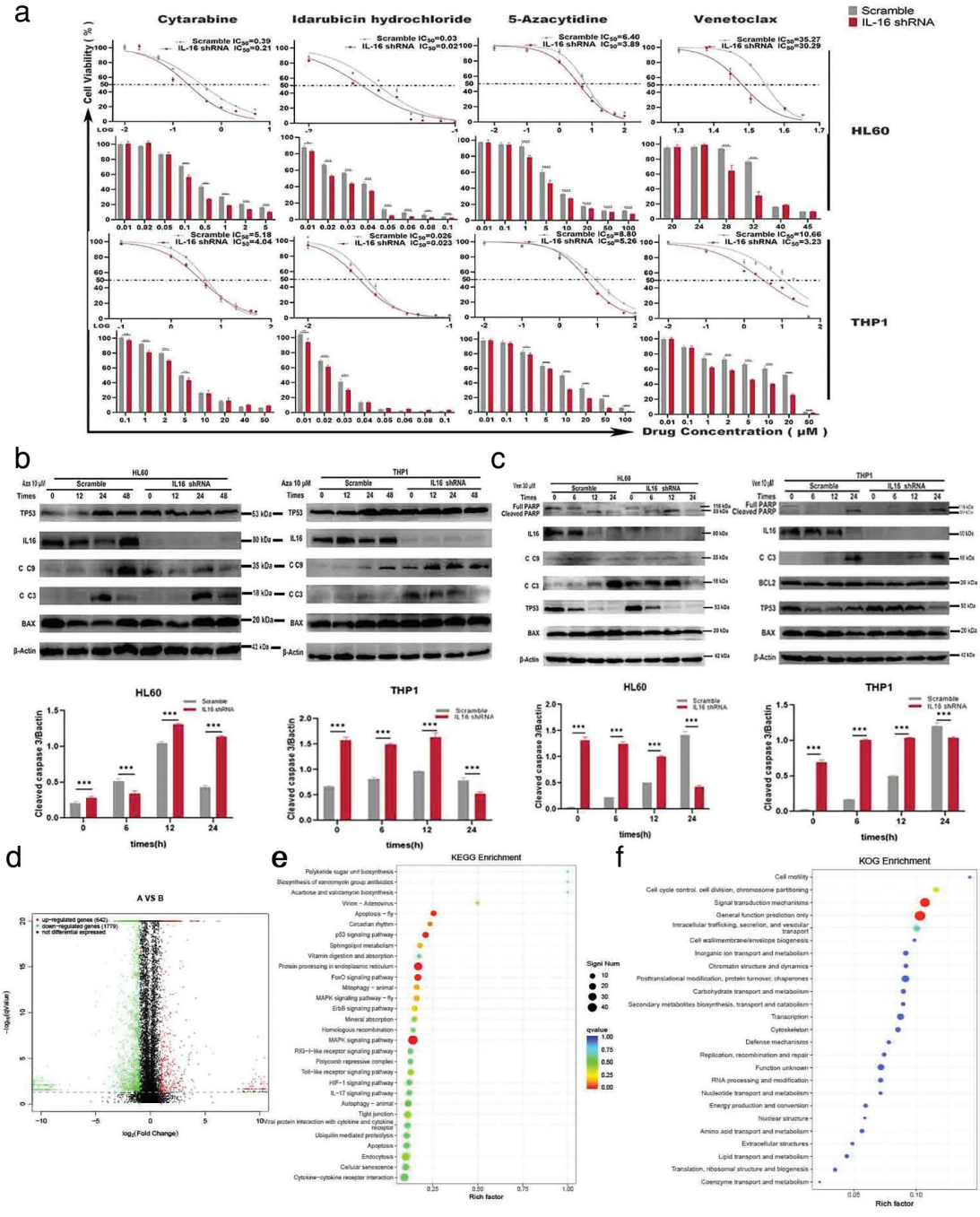

FIG. 4. Knockdown of *IL16* may overcome resistance of AML cells to multiple chemotherapeutic drugs. THP1 and HL60 cells were transfected with *IL16* shRNA constructs to knockdown *IL16* expression. (a) Sigmoid curves showing IC_{50} of different chemotherapeutic drugs after 48 h in scramble and *IL16*-shRNA transfected cells. Bar graphs showing the percentage of apoptotic and surviving cells at different drug concentrations with mean values ± SD, n = 3. (b) Western blot analysis of TP53, *BAX*, cleaved caspase 9 (C C9) and cleaved caspase 3 (C C3) was carried out on scramble and *IL16*-shRNA transfected THP1 and HL60 cells after AZA treatment. bar charts show expressed as cleaved caspase/β-actin intensity with mean ± SD, n = 3. (c) Western blot analysis of *TP53*, PARP/cleaved PARP, *BAX*, C C9 and C C3 was carried out on scramble and *IL16*-shRNA transfected HL60 cells and THP1 cell after Ven treatment. bar charts show expressed as cleaved caspase β-actin intensity with mean ± SD, n = 3. Mann-Whitney U test $*p < 0.05$, $**p < 0.01$, $***p < 0.001$. (d) Volcano plot of differentially expressed genes between HL60-shScramble and HL60-shRNA1. (e, f) Annotation of KEGG pathway and KOG of the differentially expressed gene between HL60-shScramble and HL60-shRNA1. *p* value < 0.05, Q value < 0.05).

IL16, interleukin 16; AML, acute myeloid leukemia; AZA, azacitidine; SD, standard deviation; KEGG, Kyoto Encyclopedia of Genes and Genomes; KOG, Clusters of Orthologous Groups; AML, acute myeloid leukemia.

Downregulation of IL16 expression reduces the half-life of mutant TP53 proteins

Due to the critical role of mutant *TP53* accumulation in chemotherapy resistance, the interaction between *IL16* and the P53 signaling pathway was further investigated. Nested PCR amplification was initially performed to confirm sequence alignment with predicted size ranges, followed by sequencing (Figure 5a). The wild-type *TP53 r*eference sequence NM_000546 from National Center for Biotechnology Information was used, and SNAPGENE software was employed for sequence analysis. Multisite *TP53* mutations were identified in HL60 and THP1 cells, with mutated amino acid positions at 72, 175, 218, 348, and 349. Specifically, a 46-base pair deletion at position 175 was observed in HL60 cells, whereas a 26-base pair deletion at the same position was detected in THP1 cells, potentially leading to frameshift mutations (Figure 5b). Sequence comparison indicated that the mutant *TP53* in THP1 aligns with previous reports (GenBank: JN601516.1), whereas the mutant T*P53* in HL60 is novel. THP1 cells were then coincubated with chemotherapeutic drugs, and Western blot analysis was performed to monitor mutant *TP53* accumulation (Figure 5c). Protein samples from scramble and *IL16* knockdown cells were collected at six time points and analyzed for mutant *TP53* expression. The results showed that mutant *TP53* expression began to decrease from 12 h onward. Gray-scale analysis of Western blots revealed a significant decrease in mutant *TP53* in HL60-*IL16*-shRNA cells at multiple time points and in THP1-*IL16*-shRNA cells at specific time points compared with scramble controls. The half-life of mutant *TP53* in *IL16* knockdown cells was 40 h, whereas no significant reduction was observed in scramble controls (Figure 5d, e). These findings provide preliminary evidence that *IL16* knockdown promotes mutant *TP53* degradation *in vitro*. Nevertheless, the precise molecular mechanisms through which *IL16* regulates mutant *TP53* stability remain to be elucidated and warrant further investigation.

DISCUSSION

Cytokine therapy is a novel therapeutic approach that modulates the plasma concentration of cytokines, thereby enhancing the activity of relevant cell subpopulations and promoting the cytotoxic effect on AML tumor cells.[22-24] IL16 has been reported to stimulate the migration of Tregs and T cells toward Foxp3-positive/negative cells.[25] T-cell differentiation toward Foxp3(+) Treg cells may contribute to the dysregulation of myeloid cell subset ratios and immune tolerance observed in chemotherapy-resistant patients with relapsed/refractory AML, a process potentially driven by the release of *IL16* from apoptotic AML tumor cells.[26]

Our bioinformatic analysis demonstrated widespread *IL16* expression in malignant cells from AML patients. Correlation analysis revealed that genes positively associated with *IL16* expression were predominantly enriched in B- and T-cell immunoregulation, cytokine signaling, and chemokine pathways. Elevated *IL16* expression was linked to the activation of immunosuppressive pathways, including those involving cytokines and chemokines. Although *IL16* expression was not significantly associated with overall survival in the analyzed datasets, a modest, non-significant increase in mortality risk was observed among patients with high *IL16* expression levels. Detection of *IL16* mRNA and protein expression in four AML cell lines *in vitro* revealed variable expression levels, with notable discrepancies between mRNA and protein. Given the pronounced heterogeneity of AML, this inconsistency may reflect differential post-transcriptional regulatory mechanisms operating in distinct cell populations. To further explore *IL16*'s functional role, stable *IL16*-knockdown cell lines were established using shRNA interference. Mitochondrial membrane potential assays demonstrated that *IL16* knockdown in HL60 and THP1 cells caused a more pronounced decrease in mitochondrial membrane potential compared with controls. As a decline in mitochondrial membrane potential is an early marker of apoptosis, these findings suggest that *IL16* downregulation enhances early apoptosis induced by AZA. Transcriptomic sequencing and bioinformatic analysis indicated that these effects are primarily mediated through modulation of the *TP53* pathway. Mutant *TP53* is a significant prognostic indicator in AML, with studies reporting a prevalence of *TP5*3 mutations in hematological malignancies, particularly in AML patients, of approximately 76%.[27] The *TP53* R248Q hotspot mutation is frequently observed in AML and is strongly associated with poor prognosis; most patients harboring this mutation succumb to the disease within months despite intensive anti-leukemic therapy.[28] Clinically employed chemotherapeutic agents have been observed to promote mutant *TP53* accumulation in THP1 cells, enhancing tumor cell drug resistance. Additionally, our findings demonstrate a significantly reduced half-life of mutant *TP53* protein in *IL16* knockdown cells compared with controls, suggesting that *IL16* downregulation facilitates mutant *TP53* degradation and may overcome chemotherapy resistance in AML cells.[29,30]

Nevertheless, this study has several limitations. Functional data were derived from *in vitro* models, which cannot fully recapitulate

TABLE 1. RNA-seq Data and Corresponding Clinical Information for AML were Obtained From the UCSC Xena Database, Including Datasets from TCGA and TARGET.

Dataset name	Database source	Data types	Number of samples
TARGET_LAML	UCSC Xena	Gene expression RNA-seq and clinical information	190
TCGA_LAML	UCSC Xena	Gene expression RNA-seq and clinical information	132
GSE116256	GEO	Single-cell RNA-seq	20

TCGA, The Cancer Genome Atlas; TARGET, Therapeutically Applicable Research to Generate Effective Treatments; USCS, University Of Cingifornia Sisha Cruz; GEO, Gene Expression Omnibus; AML, acute myeloid leukemia.

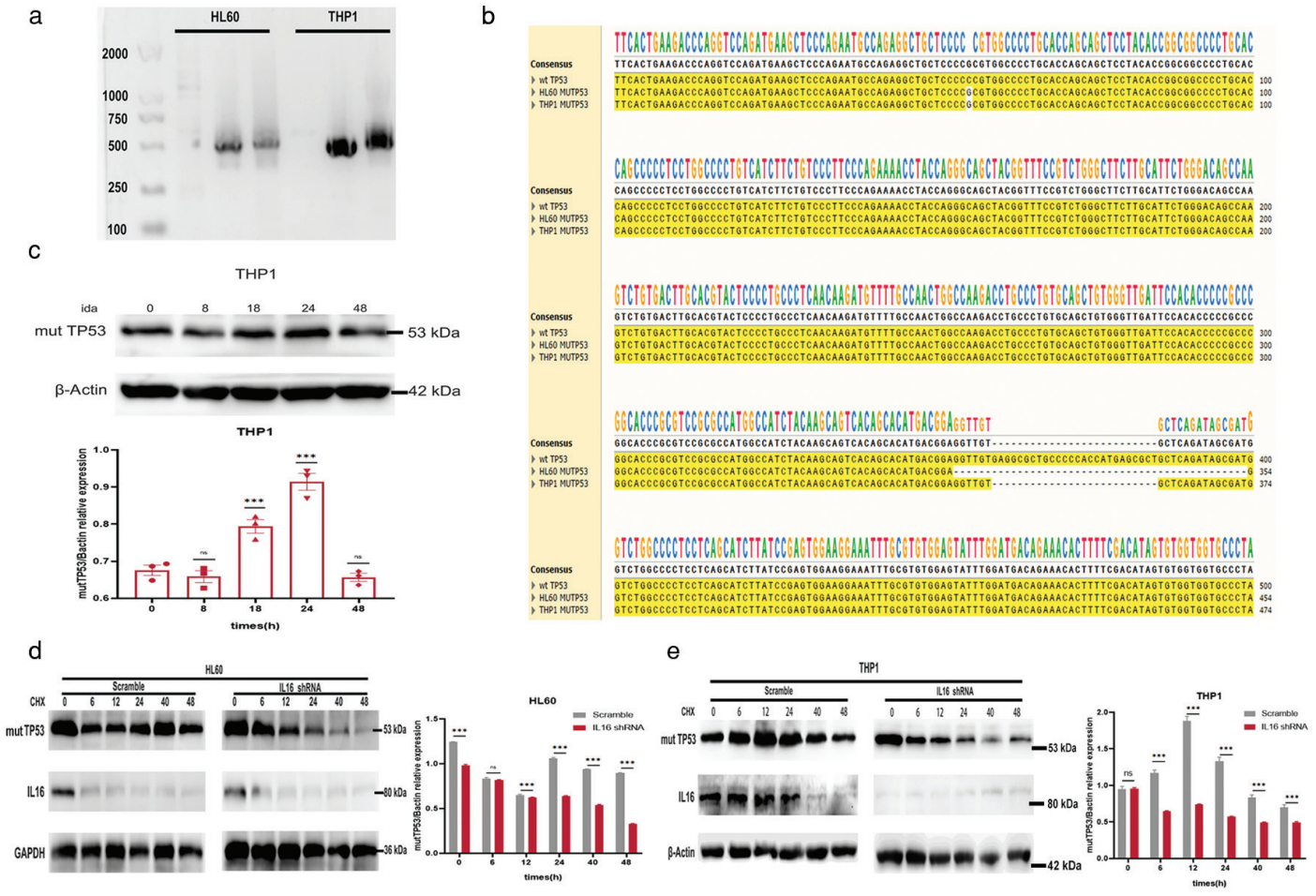

FIG. 5. Downregulation of *IL16* reduces the half-life of mutant *TP53* proteins. (a) Nested PCR showed p53 in HL60 and THP1. (b) Sequence comparison of P53 with wild-type P53 from HL60 and THP1 cell lines using SNAPGENE software. (c) Mut P53 Protein expression levels were detected by Western blot after 0, 8, 18, 24 and 48 h co-incubation of Ida in THP1, Mut *TP53*/β-actin intensity with mean ± SD, n = 3. (d, e) Western blot analysis of Mut P53 was carried out on scramble and *IL16* construct transfected HL60 (d) and THP1 (e) cells after Cycloheximide, CHX (100ug/mL) treatment. Bar charts show expressed as Mut P53/β-actin intensity with mean ± SD, n = 3. Mann-Whitney U test *$p < 0.05$, **$p < 0.01$, ***$p < 0.001$.

IL16, interleukin 16; SD, standard deviation;. PCR, polymerase chain reaction.

the *in vivo* tumor environment. The precise molecular mechanism by which *IL16* stabilizes mutant *TP53* remains unclear. Future studies using primary patient samples, animal models, and clinical cohorts are essential to assess the therapeutic potential of targeting this pathway. Additionally, due to the modest sample size and lack of formal power analysis, the statistical power of the study is limited, and the findings should be interpreted as exploratory observations that warrant validation in larger cohorts. In summary, chemotherapy-induced apoptosis in AML cells is accompanied by upregulation and release of active *IL16*. Targeting *IL16* enhances apoptosis via mechanisms involving the *TP53* pathway and may overcome multiple forms of chemotherapy resistance.

Acknowledgments: The authors thank the TCGA and GEO databases for sharing the AML sequencing dataset. And corresponding survival profiles. We are grateful to the First Hospital of Guangzhou Medical University for the provision of the experimental platform.

Ethics Committee Approval: Not applicable.

Informed Consent: Not applicable.

Data Sharing Statement: The data that support the findings of this study are available from the corresponding authors upon reasonable request.

Authorship Contributions: Concept- H.Z., Z.H., S.D., L.X.; Design- H.L., L.X.; Supervision- H.L., L.X.; Funding- Z.H., S.Y., L.X.; Data Collection or Processing- H.Z., P.Q., A.L.; Analysis and/or Interpretation- H.Z., P.Q.; Literature Review- H.Z., S.Y.; Writing- H.Z.

Conflict of Interest: The authors declare that they have no conflict of interest.

Funding: This study was supported by Guangzhou Science and Technology Project (2023A03J0347, 2024A03J1149, 2023A03J0348).

Supplementary Tables: https://balkanmedicaljournal.org/img/files/balkan-2026.2025-12-245-supplemantry-r.pdf

Supplementary Figure: https://balkanmedicaljournal.org/img/files/balkan-2026.2025-12-245-supplemantry-figure%281%29.pdf

REFERENCES

1. DiNardo CD, Erba HP, Freeman SD, Wei AH. Acute myeloid leukaemia. *Lancet*. 2023;401:2073-2086. [CrossRef]
2. Siegel RL, Miller KD, Wagle NS, Jemal A. Cancer statistics, 2023. CA Cancer J Clin. 2023;73:17-48. [CrossRef]
3. Cruikshank WW, Kornfeld H, Center DM. Interleukin-16. *J Leukoc Biol*. 2000;67:757-766. [CrossRef]
4. Zhang XM, Xu YH. The associated regulators and signal pathway in rIL-16/CD4 mediated growth regulation in Jurkat cells. *Cell Res*. 2002;12:363-372. [CrossRef]
5. Cruikshank WW, Kornfeld H, Center DM. Signaling and functional properties of interleukin-16. *Int Rev Immunol*. 1998;16:523-540. [CrossRef]
6. Okubo Y, Tsukadaira A, Takashi S, Kubo K, Koyama S. Chemotaxis of human CD4+ eosinophils. *Int Arch Allergy Immunol*. 2001;125 Suppl 1:19-21. [CrossRef]
7. Zhang Y, Kornfeld H, Cruikshank WW, Kim S, Reardon CC, Center DM. Nuclear translocation of the N-terminal prodomain of interleukin-16. *J Biol Chem*. 2001;276:1299-1303. [CrossRef]
8. Wilson KC, Center DM, Cruikshank WW. The effect of interleukin-16 and its precursor on T lymphocyte activation and growth. *Growth Factors*. 2004;22:97-104. [CrossRef]
9. Richmond J, Tuzova M, Cruikshank W, Center D. Regulation of cellular processes by interleukin-16 in homeostasis and cancer. *J Cell Physiol*. 2014;229:139-147. [CrossRef]
10. Atanackovic D, Hildebrandt Y, Templin J, et al. Role of interleukin 16 in multiple myeloma. J *Natl Cancer Inst*. 2012;104:1005-1020. [CrossRef]
11. Center DM, Cruikshank WW, Zhang Y. Nuclear pro-IL-16 regulation of T cell proliferation: p27(KIP1)-dependent G0/G1 arrest mediated by inhibition of Skp2 transcription. J *Immunol*. 2004;172:1654-1660. [CrossRef]
12. Cruikshank W, Little F. Interleukin-16: the ins and outs of regulating T-cell activation. *Crit Rev Immunol*. 2008;28:467-483. [CrossRef]
13. Guan X, Wang Y, Fang T, et al. Lymphoma cell-driven IL-16 is expressed in activated B-cell-like diffuse large B-cell lymphomas and regulates the pro-tumor microenvironment. *Haematologica*. 2025;110:425-438. [CrossRef]
14. Mumme HL, Raikar SS, Bhasin SS, et al. Single-cell RNA sequencing distinctly characterizes the wide heterogeneity in pediatric mixed phenotype acute leukemia. *Genome Med*. 2023;15:83. [CrossRef]
15. Wu X, Thisdelle J, Hou S, et al. Elevated expression of interleukin 16 in chronic lymphocytic leukemia is associated with disease burden and abnormal immune microenvironment. *Leuk Res*. 2023;131:107315. [CrossRef]
16. Andersen BL, Goyal NG, Weiss DM, et al. Cells, cytokines, chemokines, and cancer stress: a biobehavioral study of patients with chronic lymphocytic leukemia. *Cancer*. 2018;124:3240-3248. d[CrossRef]
17. Tang Z, Li C, Kang B, Gao G, Li C, Zhang Z. GEPIA: a web server for cancer and normal gene expression profiling and interactive analyses. *Nucleic Acids Res*. 2017;45:W98-W102. [CrossRef]
18. Goldman MJ, Craft B, Hastie M, et al. Visualizing and interpreting cancer genomics data via the Xena platform. *Nat Biotechnol*. 2020;38:675-678. [CrossRef]
19. Subramanian A, Tamayo P, Mootha VK, et al. Gene set enrichment analysis: a knowledge-based approach for interpreting genome-wide expression profiles. *Proc Natl Acad Sci U S A*. 2005;102:15545-15550. [CrossRef]
20. van Galen P, Hovestadt V, Wadsworth Ii MH, et al. Single-Cell RNA-Seq reveals AML hierarchies relevant to disease progression and immunity. *Cell*. 2019;176:1265-1281. e24. [CrossRef]
21. Miao Y, Du Q, Zhang HG, Yuan Y, Zuo Y, Zheng H. Cycloheximide (CHX) chase assay to examine protein half-life. *Bio Protoc*. 2023;13:e4690. [CrossRef]
22. Shaffer BC, Gillet JP, Patel C, Baer MR, Bates SE, Gottesman MM. Drug resistance: still a daunting challenge to the successful treatment of AML. Drug Resist Updat. 2012;15:62-69. [CrossRef]
23. Niewold TB, Lehman JS, Gunnarsson I, Meves A, Oke V. Role of interleukin-16 in human diseases: a novel potential therapeutic target. *Front Immunol*. 2025;16:1524026. [CrossRef]
24. Karimdadi Sariani O, Eghbalpour S, Kazemi E, Rafiei Buzhani K, Zaker F. Pathogenic and therapeutic roles of cytokines in acute myeloid leukemia. *Cytokine*. 2021;142:155508. [CrossRef]
25. Fang W, Shi C, Wang Y, Song J, Zhang L. microRNA-128-3p inhibits CD4+ regulatory T cells enrichment by targeting interleukin 16 in gastric cancer. *Bioengineered*. 2022;13:1025-1038. [CrossRef]
26. Skundric DS, Cruikshank WW, Drulovic J. Role of IL-16 in CD4+ T cell-mediated regulation of relapsing multiple sclerosis. *J Neuroinflammation*. 2015;12:78. [CrossRef]
27. Tashakori M, Kadia T, Loghavi S, et al. TP53 copy number and protein expression inform mutation status across risk categories in acute myeloid leukemia. *Blood*. 2022;140:58-72. [CrossRef]
28. Daver NG, Maiti A, Kadia TM, et al. TP53-mutated myelodysplastic syndrome and acute myeloid leukemia: biology, current therapy, and future directions. *Cancer Discov*. 2022;12:2516-2529. Erratum in: *Cancer Discov*. 2022;12:2954. [CrossRef]
29. Shin DY. *TP53* mutation in acute myeloid leukemia: an old foe revisited. *Cancers (Basel)*. 2023;15:4816. [CrossRef]
30. Chen X, Zhang T, Su W, et al. Mutant p53 in cancer: from molecular mechanism to therapeutic modulation. *Cell Death Dis*. 2022;13:974. [CrossRef]